"Back Door" Opening Implied by the Crystal Structure of a Carbamoylated Acetylcholinesterase‡

Cecilia Bartolucci,§,|| Emanuele Perola,§,|| Luciano Cellai,§ Mario Brufani,⊥ and Doriano Lamba*,@

Istituto di Strutturistica Chimica "G. Giacomello", CNR, P.O. Box 10, I-00016 Monterotondo Stazione, Rome, Italy, Dipartimento di Scienze Biochimiche "A. Rossi-Fanelli", Università degli Studi di Roma "La Sapienza", Via degli Apuli 9, I-00185 Rome, Italy, and International Centre for Genetic Engineering and Biotechnology, Area Science Park, Padriciano 99, I-34012 Trieste, Italy

Received November 16, 1998; Revised Manuscript Received February 5, 1999

ABSTRACT: The crystal structure of *Torpedo californica* (*Tc*) acetylcholinesterase (AChE) carbamoylated by the physostigmine analogue 8-(*cis*-2,6-dimethylmorpholino)octylcarbamoyleseroline (MF268) is reported at 2.7 Å resolution. In the X-ray structure, the dimethylmorpholinooctylcarbamic moiety of MF268 is covalently bound to the catalytic serine, which is located at the bottom of a long and narrow gorge. The alkyl chain of the inhibitor fills the upper part of the gorge, blocking the entrance of the active site. This prevents eseroline, the leaving group of the carbamoylation process, from exiting through this path. Surprisingly, the relatively bulky eseroline is not found in the crystal structure, thus implying the existence of an alternative route for its clearance. This represents indirect evidence that a "back door" opening may occur and shows that the release of products via a "back door" is a likely alternative for this enzyme. However, its relevance as far as the mechanism of substrate hydrolysis is concerned needs to be established. This study suggests that the use of properly designed acylating inhibitors, which can block the entrance of catalytic sites, may be exploited as a general approach for investigating the existence of "back doors" for the clearance of products.

Acetylcholinesterase plays a fundamental role in the regulation of impulse transmission, terminating the action of the neurotransmitter acetylcholine at cholinergic synapses and neuromuscular junctions (*1*). AChE[1] inhibitors are widely employed both in the symptomatic treatment of diseases involving acetylcholine depletion, like Alzheimer's disease (AD), glaucoma, and myastenia gravis, and as insecticides for agricultural purposes (*2*). AChE is one of the most efficient enzymes studied so far, and its catalytic mechanism, although thoroughly studied, is still the object of thorough investigation.

The crystal structure of AChE from *Tc* (*3*) revealed that the active site, constituted by a catalytic triad and a so-called anionic subsite, is located at the bottom of a deep and narrow gorge. The anionic subsite recognizes the quaternary ammonium group of the substrate, while the catalytic triad, formed by Glu327, His440, and Ser200, is responsible for its resultant hydrolysis. At the entrance of the gorge, there is a regulatory site called the "peripheral anionic site". There is structural evidence that residues Trp84 and Trp279 play a central role in the catalytic and peripheral anionic sites, respectively (*4*). The presence of a strong electrostatic dipole directed toward the bottom of the gorge has been elucidated (*5*). Such a dipole should be unfavorable to the clearance of the cationic product choline, in apparent contrast with the high catalytic rate of the enzyme. The presence of a "back door" at the bottom of the catalytic pocket has been hypothesized (*5*), and its actual existence is still the object of a great controversy (*6*, *7*).

A good deal of structural evidence of the complexes between the enzyme and its reversible inhibitors is now available. Since 1993, the crystal structures of complexes between *Tc* AChE and tacrine (*4*), edrophonium (*4*, *8*), decamethonium (*4*), fasciculin (*9, 10*), huperzine A (*11*), and E2020 (*12*) have been determined. The structure of a complex with μ-(*N*,*N*′,*N*′′-trimethylammonium) trifluoroacetophenone, resembling the transition state of acetylcholine hydrolysis, has also been determined (*13*), providing insights into the catalytic process. Nevertheless, there is still a lack of structural evidence for the complexes between AChE and its pseudoirreversible and irreversible inhibitors. Among these, the analogues of physostigmine, an alkaloid extracted from a tropical plant, have been widely studied as potential drugs for AD (*14*−*16*). These compounds belong to a large class of carbamate-like AChE inhibitors, whose mechanism of action is characterized by a fast carbamoylation of the catalytic serine followed by a slow regeneration of the active

‡ Crystallographic coordinates and observed structure factors have been deposited at the Brookhaven Protein Data Bank (file names 1oce and r1ocesf, respectively).

* To whom correspondence should be addressed: International Centre for Genetic Engineering and Biotechnology, Area Science Park, Padriciano 99, I-34012 Trieste, Italy. Phone: +39-040-226881 or +39-040-3757354. Fax: +39-040-9221126 or +39-040-226555. E-mail: lamba@icgeb.trieste.it or lamba@cnrelt.area.trieste.it.

§ Istituto di Strutturistica Chimica "G. Giacomello".

|| C.B. and E.P. contributed equally to this work.

⊥ Università degli Studi di Roma "La Sapienza".

@ International Centre for Genetic Engineering and Biotechnology.

[1] Abbreviations: *Tc*, *Torpedo californica*; AChE, acetylcholinesterase; MF268, 8-(*cis*-2,6-dimethylmorpholino)octylcarbamoyleseroline; AD, Alzheimer's disease.

10.1021/bi982723p CCC: $18.00
Published on Web 04/15/1999

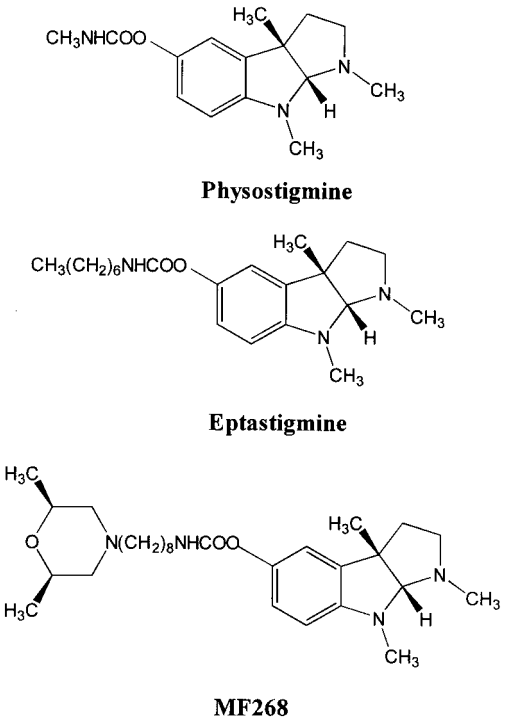

FIGURE 1: Chemical structures of physostigmine, eptastigmine, and MF268.

enzyme (*17*). The process is similar to that of substrate hydrolysis, which differs due to the immediate reactivation of the acylated enzyme. The structure of a stable carbamoylated enzyme would provide an analogue of the intermediate of acetylcholine hydrolysis, and it would shed light on both the catalytic mechanism of AChE and the inhibition process for this class of compounds.

While the enzyme inhibited by physostigmine is reactivated in vitro with a $t_{1/2}$ of 39 min at 25 °C, long chain physostigmine analogues form much more stable adducts with the enzyme; the reactivation of AChE inhibited by eptastigmine (Figure 1), which is presently in phase III clinical trial as anti-AD drug, occurs in vitro with a $t_{1/2}$ of several days at 25 °C. A more recent semisynthetic analogue, MF268, which carries a dimethylmorpholino group at the end of the alkyl chain, forms an even more stable adduct with AChE, behaving in vitro as a practically irreversible inhibitor (*18*). Such stability led us to choose the complex AChE−MF268 as the ideal candidate for the planned structural studies.

We now report the 2.7 Å crystal structure of this complex, which represents the first direct evidence of carbamoylated AChE, and sheds light on two important widely debated questions: the location of the leaving group after the carbamoylation step, with implications concerning the actual existence of a "back door" in the catalytic pocket, and the reasons for the great stability to hydrolysis of long chain carbamoylated adducts of AChE.

MATERIALS AND METHODS

Crystallization. MF268 was kindly provided by Mediolanum Farmaceutici (Milano, Italy). AChE from *Tc* was extracted, purified, and crystallized as previously described (*19*). Crystals grew in 2−3 weeks up to a size of 150 μm × 150 μm × 200 μm. The crystals of the complex AChE−MF268 were obtained by soaking the native crystals at 4 °C in 3 mM MF268, 42% PEG200, and 0.1 M MES at pH 6.0 for 3 days.

Structure Determination. X-ray diffraction data were collected with a 180 mm MAR Research imaging plate (X-ray Research, Hamburg, Germany) at the HXRD beam line of the Italian Synchrotron facility ELETTRA (Trieste, Italy). The crystals were flash-cooled at 120 K, using an Oxford Cryosystems cooling device (Oxford, U.K.), by being transferred directly from the soaking solution to a stream of boiled off nitrogen. The diffraction pattern of the crystals of the AChE−MF268 complex is anisotropic, with reflections observed along the best and worst directions at 2.5 Å and 3.0 Å Bragg spacing. Data processing was carried out with DENZO, SCALEPACK (*20*), and the CCP4 package (*21*). The refined coordinates of the native *Tc* AChE (*11*) [PDB file name 2ace (*22*)] were used after removal of the water molecules to calculate the initial phases for the enzyme−inhibitor structure. This model was used in the anisotropic scaling of the data with X-PLOR 3.851 (*23*). The structure factor σ values were also rescaled appropriately, and the corrected data were used for all subsequent procedures. The structure was determined by the difference Fourier technique. The inhibitor was built with the program SYBYL (Tripos, Inc.). The X-PLOR program was used for crystallographic refinement. For the complex, $2F_o - F_c$ and $F_o - F_c$ maps were computed after initial refinement of the native protein by simulated annealing (at a maximum temperature of 3000 K), followed by conjugate gradient minimization and restrained individual atomic temperature factor refinement. A prominent difference electron density feature in the catalytic gorge allowed unambiguous fitting of the dimethylmorpholinooctylcarbamic moiety of the MF268 inhibitor, covalently bound to O^{γ} of Ser200. Peaks in the difference Fourier maps that were greater than 2.5σ and that displayed good hydrogen-bonding geometry with respect to the protein were built in as solvent molecules. Map inspection and model correction during refinement were carried out with the graphics program O (*24*). The statistics of crystallographic analysis and refinement are shown in Table 1. The probe accessible volume for the active site of *Tc* AChE was calculated using VOIDOO (version 3.1.2) (*26*). The radius of the probe was 1.4 Å, and each calculation was refined for 10 cycles.

RESULTS AND DISCUSSION

The overall structure of the AChE−MF268 complex does not display significant conformational changes when compared to the structure of the free enzyme (*11*). The presence of a long chain molecule within the active site gorge is clearly shown by an elongated electron density, which starts in the proximity of the side chain of Ser200 and terminates near the indole ring of Trp279 (Figure 2a). The contour of the map clearly defines the shape of the dimethylmorpholinooctylcarbamic moiety of the inhibitor, which appears to be covalently bound to O^{γ} of Ser200. The presence of a C−O covalent bond is confirmed by the distance of 1.4 Å between the atoms involved, which results from the refinement without any external restraint. The carbamic group is stabilized by hydrogen bonds between the carbonyl oxygen and the N−H functions of Gly118 and Gly119, belonging to the so-called oxy anion hole (*3*), the respective O−N distances being 2.7 and 2.9 Å.

Table 1: Crystal, Data Collection, and Refinement Statistics of the AChE−MF268 Complex

Crystal Parameters	
space group	$P3_121$
cell dimensions	$a = b = 111.50$ Å, $c = 137.39$ Å, $\alpha = \beta = 90°$, $\gamma = 120°$
Data Collection	
X-ray source	HXRD, ELETTRA, Trieste, Italy
wavelength (Å)	0.92
temperature (K)	120.0
resolution range (Å)	20.0−2.7 (2.8−2.7)[a]
no. of measurements	248837
no. of unique reflections [$I \geq 0\sigma$(I)]	24043 (1886)
completeness (%)	87.2 (69.7)
multiplicity	2.3 (1.6)
R_{sym}[b] (%)	14.0 (64.8)
mean I/σ(I) of merged data	6.7 (1.7)
Refinement Statistics	
resolution used (Å)	8.0−2.7
no. of reflections used [$F_o \geq 2\sigma(F_o)$]	22426
R_{cryst}, R_{free}[c] (%)	20.8, 29.1
rmsd for bond lengths[d] (Å)	0.008
rmsd for bond angles[d] (deg)	1.3
no. of atoms	
protein	205
water	157
inhibitor	19
all atoms	4381
average temperature factors (Å^2)	
protein	29.0
water	34.9
inhibitor	39.9
all atoms	29.3
rmsd for ΔB[e] (Å^2)	1.90

[a] Numbers in parentheses refer to the shell of highest-resolution data. [b] $R_{sym}(I) = \Sigma_{hkl}\Sigma_i|I_{hkl,i} - \langle I_{hkl}\rangle|/\Sigma_{hkl}\Sigma_i|I_{hkl,i}|$, with $\langle I_{hkl}\rangle$ being the mean intensity of the multiple $I_{hkl,i}$ observations from symmetry-related reflections. [c] $R_{cryst} = \Sigma_{hkl}|F_o - F_c|/\Sigma_{hkl}F_o$, where F_o and F_c are the observed and calculated structure factor amplitudes for reflection *hkl*, respectively. The R_{free} was calculated by randomly omitting 5% of the observed reflections from the data set. [d] Stereochemical criteria are those of Engh and Huber (*25*). [e] rmsd for ΔB is the rmsd of the ΔB factor of bonded atoms.

This is the first structural evidence of carbamoylated acetylcholinesterase, a species which is known to form in the mechanism of action of all carbamate-like inhibitors (*17*). The presence of a homogeneously carbamoylated enzyme in the crystals demonstrates that the long duration of action of MF268 must be ascribed to the stability of the carbamoylated adduct.

The structure shows that the dimethylmorpholinooctyl moiety enables the inhibitor to bridge the catalytic and peripheral anionic site of the enzyme. As shown in Figure 2b, the morpholine ring is opposed to the indole system of Trp279, the main component of the peripheral site, as are one of the quaternary groups of decamethonium and the indanone moiety of E2020 in the corresponding complexes with AChE (*4*, *12*). Analogously, a cation−π interaction (*27*, *28*) can be identified, occurring in this case between the basic amino group of morpholine and the indole ring of Trp279. This interaction enhances the affinity of MF268 for AChE, thus accounting for its higher inhibitory potency compared to that of eptastigmine (*18*).

The superimposition of the structures of the decamethonium (*4*) and MF268 complexes (Figure 2b) shows a similar spatial disposition of the interacting nitrogens with respect to Trp279; the distances from N to the center of the indole ring are 4.7 and 5.6 Å for decamethonium and MF268, respectively. A comparison of the conformation of MF268 with that of decamethonium in Figure 2b shows then that the alkyl chains, both displaying a mixture of trans and gauche rotamers, partially overlap in the upper part of the catalytic gorge. In the lower part, the alkyl chain of MF268 bends toward the catalytic serine, while the chain of decamethonium points directly to the Trp84 of the anionic subsite, thus holding a more linear and extended conformation.

Because of the long and narrow active site, MF268 can only reach the catalytic site with an extended conformation. The eseroline moiety, carrying two basic amino groups, is responsible for the recognition of the anionic subsite, as is the quaternary group of the substrate. On the basis of the observed structural features, it is plausible that the interaction between the eseroline moiety and Trp84, occurring at the bottom of the gorge, induces the alkyl chain to bend and, as a result, the carbamic moiety to assume an orientation that is suitable for the nucleophilic attack by the catalytic serine.

In the carbamoylation process by AChE, eseroline is the leaving group. In the $2F_o - F_c$ map, a residual electron density is present in the proximity of Trp84. The shape and dimensions of the eseroline molecule do not fit into the space defined by this density, which instead can properly accommodate two water molecules, also observed in the structure of the native enzyme (*11*). The leaving group eseroline is then cleared from the active site in the present complex.

The evaluation of the solvent accessible molecular surface of the complex (probe radius of 1.4 Å) shows that the alkyl chain of the inhibitor totally blocks the access to the active site. In the crystal structure as such, even the diffusion of a water molecule to and from the active site is not sterically feasible. This would imply the occurrence of alternative routes, connecting the catalytic pocket with the protein surface, for the release of eseroline. The following considerations provide strong support for this hypothesis.

(1) The results from molecular dynamics simulations of a AChE dimer complexed with tacrine (*29*) revealed fluctuations in the width of the primary channel that would barely allow the access of the substrate acetylcholine to the catalytic site. Eseroline is bulkier than acetylcholine, and it cannot assume a planar structure. Therefore, its diffusion through the gorge, in the presence of an alkyl chain, seems to be very unlikely. (2) The present experiment is performed in the crystalline state, in which the conformational freedom is reduced if compared to that of the solution state. As a result, the fluctuations within the catalytic pocket are even more limited. It is extremely unlikely that, in the crystalline state, the movements in the pocket can be wide enough to allow eseroline to be released across the gorge. (3) The narrowness of the gorge is at the basis of the substrate specificity of acetylcholinesterase; larger inhibitors, like propidium, are confined at the peripheral site (*30*). No inhibitor with a cross section comparable to that of eseroline with an alkyl chain is known to interact with the catalytic site at the bottom of the gorge.

In view of these considerations, the structure of the AChE−MF268 complex represents indirect evidence that "back door" release of the hydrolysis product may occur in this case.

As mentioned above, a "back door" hypothesis for the clearance of choline was raised to clarify the apparent

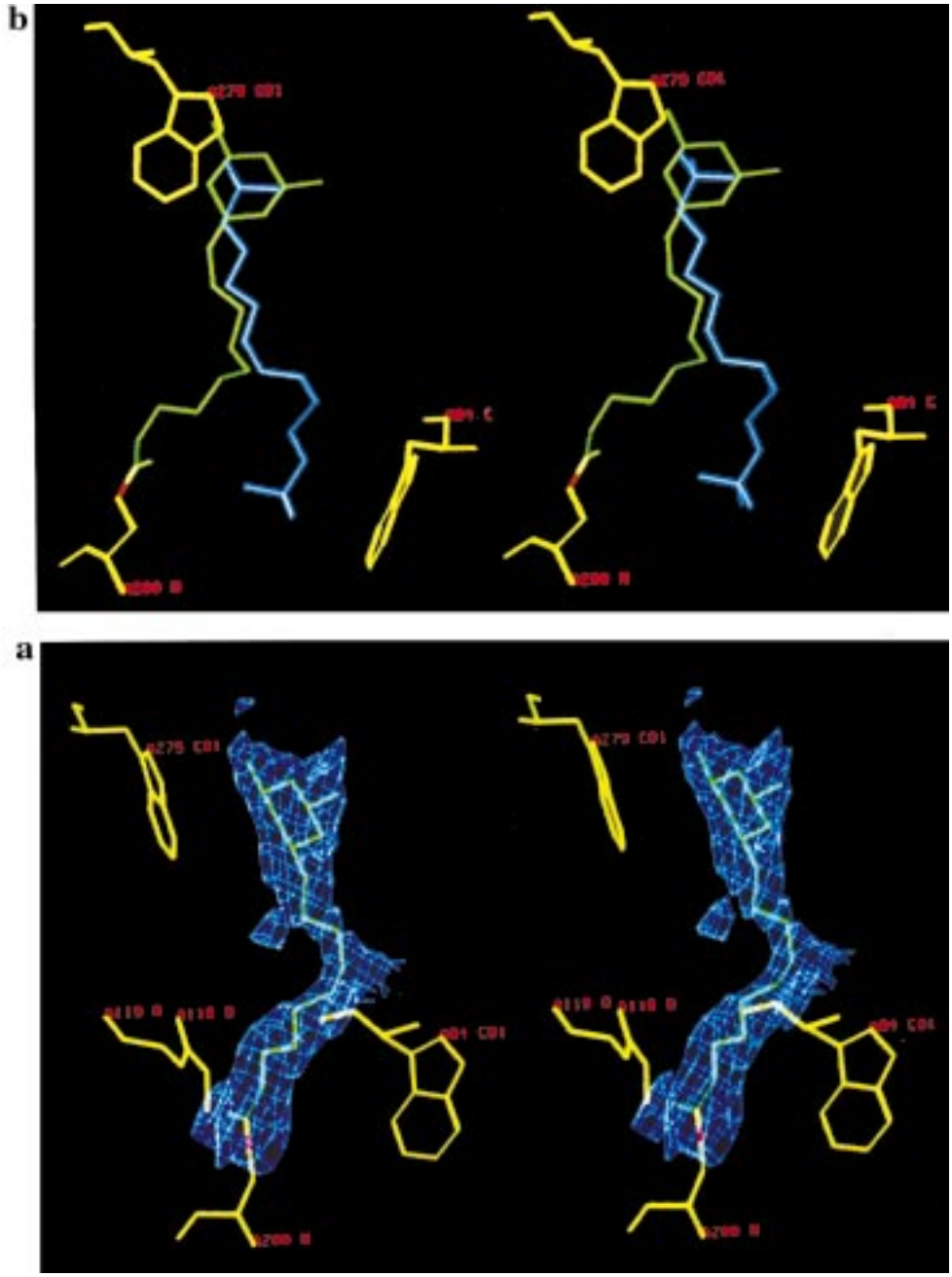

FIGURE 2: (a) Stereoview of the initial difference ($2F_o - F_c$) electron density map of the complex. The map is countered at 1.0σ, and the final model of the dimethylmorpholinooctylcarbamic moiety is green. Selective active site residues are indicated. (b) A perspective stereoview of the catalytic site and the inhibitor molecules in the superimposed refined structures of the *Tc* AChE complexes with decamethonium (blue) (*4*) and MF268 (green), respectively. The backbone superimposition of the complexes was created using the LSQ option in O (*24*); diagrams were generated with the program O (*24*).

contrast between the high catalytic rate of the enzyme and the presence of a strong electrostatic dipole in the gorge, which should be unfavorable for the exit of a cation from the mouth of the gorge itself (*3*). On the basis of a molecular dynamics simulation of *Tc* AChE, the transient opening of a channel in the proximity of Trp84, which would allow the clearance of choline, was exhibited (*5*).

Two possible ways of generating the channel were proposed: a shutter-like in-plane motion of Trp84, Val129, and Gly441 and a flap-like conformational transition of the Ω-loop stretching from Cys67 to Cys94. Subsequent experiments of mutagenesis failed to demonstrate the influence of such a "back door" on the catalytic activity of AChE (*6*, *7*). Mutations resulting in a strong decrease in the conformational flexibility in the putative region did not significantly affect the rate of substrate hydrolysis. However, these results did not completely exclude the occurrence of a transient opening. In fact, molecular dynamics simulations demonstrated that, despite the introduction of a disulfide bridge which tethered the Ω-loop to the body of the enzyme, the substantial conformational flexibility in the proximity of Trp84 was retained (*7*).

The present crystal structure determination cannot provide a definitive answer to this debate for two reasons. (1) The time scale of the crystallographic experiment is far too long to be compared to that of the substrate hydrolysis and hence to support a mechanistically significant "back door" release of choline. In other words, the experiment shows that, when

the main entrance of the catalytic pocket is blocked, the product can still diffuse out toward the solvent in the course of the 3 days of soaking of the crystals. However, it does not prove that the "back door" release is faster, and therefore more favorable, than the "main door" release, when the access to the active site is not hindered. (2) Eseroline is bulkier than choline, and it can hardly be accommodated in the residual cavity present in the AChE−MF268 complex. In fact, the residual volume available at the bottom of the gorge is 605 Å^3, while the solvent-excluded volume of eseroline is 637 Å^3. Therefore, at the moment of the carbamoylation, a simultaneous conformational rearrangement, necessary to make room to eseroline, must be induced, and the "back door" opening could be the consequence of such transient adaptation. The accommodation of the smaller choline does not require a similar adjustment.

These points prevent us from making a straight connection between the implications derived from this study and the catalytic mechanism of the enzyme. Nonetheless, this result shows that "back door" release of products is a feasible alternative for this enzyme, and provides the basis for further investigations with the mechanism that is involved. A time-resolved crystallographic experiment could be a valuable tool for elucidating this process.

The stability of the long chain carbamoylated adducts, which is at the basis of this study, can also be explained by the present structure. The kinetics of decarbamoylation is mainly regulated by a number of factors, such as the electrophilicity of the carbamic group and the availability of reactive water molecules in the catalytic gorge. In this case, the much slower hydrolysis of the long chain adducts with respect to the methylcarbamoylated enzyme, generated by the reaction with physostigmine, cannot be explained by electronic factors. Indeed, the electron-donating effect of a linear alkyl chain is only slightly higher than that of a methyl group, and its influence on the electrophilicity of the carbamic group is not sufficient to provide a significantly stronger stabilization against the nucleophilic attack of water. Concerning the second factor, in the structure presented here a strong depletion of the water content within the gorge is observed as compared to that of the free enzyme (*11*). In the structure of the latter, 16 evenly distributed water molecules were located within the catalytic gorge. In the complex described here, the alkyl chain completely displaces the water molecules in the upper part of the gorge, while only eight molecules can be found at the bottom of the cavity. Six of them are involved in hydrogen bonds with the residues lining the gorge, while the remaining two are hydrogen bonded to each other, and are involved in dipole−dipole interactions with the π-system of Trp84, the average distance between the oxygen atoms and the center of the indole ring being 4.9 Å. Therefore, the structure provides evidence of a scarce availability of potentially reactive water molecules in the gorge. Furthermore, as already pointed out, the access to the active site is hindered by the presence of the alkyl chain, so the diffusion of new water molecules toward the catalytic serine is also strongly limited.

The already hypothesized occurrence of transient openings in the enzyme surface could provide alternative routes to the access of solvent molecules to the active site, as also supported by molecular dynamics simulations of the AChE dimer complexed with tacrine (*29*). As observed above, the features of the electron density map of the present complex do not support the existence of highly flexible regions, which would be likely to be involved in the statistical generation of large openings. Despite this, the generation of small channels, sufficient to allow the access of water molecules, cannot be excluded, especially in a dynamic environment. This possibility would contrast with the apparent irreversibility of AChE carbamoylation by MF268. Nevertheless, the structure allows us to envisage an additional factor to explain the stability of the complex. The hydrolysis of the serine−carbamate bond would release a long chain fragment, still containing a carbamic acidic group susceptible to nucleophilic attack. The cation−π interaction between the dimethylmorpholino group and Trp279, together with the hydrophobic interactions between the alkyl chain and the aromatic residues lining the gorge, would prevent a fast clearance of this fragment from the catalytic pocket. The persistence of dimethylmorpholinooctylcarbamic acid inside the pocket would then allow a new nucleophilic addition by the reactivated catalytic triad, with restoration of the carbamoylated enzyme.

Overall, the substantial irreversibility of the inhibitory effect of MF268 can be ascribed both to the limited access of hydrolytic water molecules to the active site and to the tendency of the hydrolyzed fragments to remain reversibly bound in the gorge, thus favoring the immediate restoration of the initial adduct. This same explanation can be extended to the high stability of all the long chain carbamoylated adducts, the differences in the reactivation rate depending upon the presence or the absence of further points of anchorage to the inner surface of the gorge (*18*).

This study is an example of how the introduction of properly designed acylating inhibitors may allow us to obtain stable intermediates of enzyme reactions, in which the entrance of the catalytic pocket is blocked. This may provide useful tools for investigating the existence of "back doors" and/or "side doors" for the clearance of products, also invoked for other enzymes such as G-actin and myosin (*31*, *32*).

ACKNOWLEDGMENT

We gratefully acknowledge Mediolanum Farmaceutici (Milano, Italy) for the gift of a sample of MF268.

REFERENCES

1. Barnard, E. A. (1974) in *The Peripheral Nervous System* (Hubbard, J. I., Ed.) pp 201−224, Plenum, New York.
2. Taylor, P. (1990) in *The Pharmacological Basis of Therapeutics* (Gilman, A. G., Nies, A. S., Rall, T. W., and Taylor, P., Eds.) 5th ed., pp 131−150, McMillan, New York.
3. Sussman, J. L., Harel, M., Frolow, F., Oefner, C., Goldman, A., Toker, L., and Silman, I. (1991) *Science 253*, 872−879.
4. Harel, M., Schalk, I., Ehret-Sabatier, L., Bouet, F., Goeldner, M., Hirth, C., Axelsen, P. H., Silman, I., and Sussman, J. L. (1993) *Proc. Natl. Acad. Sci. U.S.A. 90*, 9031−9035.
5. Gilson, M. K., Straatsma, T. P., McCammon, J. A., Ripoll, D. R., Faerman, C. H., Axelsen, P. H., Silman, I., and Sussman, J. L. (1994) *Science 263*, 1276−1278.
6. Kronman, C., Ordentlich, A., Barak, D., Velan, B., and Shafferman, A. (1994) *J. Biol. Chem. 269*, 27819−27822.
7. Faerman, C., Ripoll, D., Bon, S., Le Feuvre, Y., Morel, N., Massouliè, J., Sussman, J. L., and Silman, I. (1996) *FEBS Lett. 386*, 65−71.

8. Ravelli, R. B. G., Raves, M. L., Ren, Z., Bourgeois, D., Roth, M., Kroon, J., Silman, I., and Sussman, J. L. (1998) *Acta Crystallogr. D54*, 1359−1366.
9. Bourne, Y., Taylor, P., and Marchot, P. (1995) *Cell 83*, 503−512.
10. Harel, M., Kleywegt, G. J., Ravelli, R. B. G., Silman, I., and Sussman, J. L. (1995) *Structure 3*, 1355−1366.
11. Raves, M. L., Harel, M., Pang, Y. P., Silman, I., Kozikowski, A. P., and Sussman, J. L. (1997) *Nat. Struct. Biol. 4*, 57−63.
12. Kryger, G., Silman, I., and Sussman, J. L. (1998) *J. Physiol. (Paris) 92*, 191−194.
13. Harel, M., Quinn, D. M., Nair, H. K., Silman, I., and Sussman, J. L. (1996) *J. Am. Chem. Soc. 118*, 2340−2346.
14. Brufani, M., Marta, M., and Pomponi, M. (1986) *Eur. J. Biochem. 157*, 115−120.
15. Craig, N. H., Pei, X. F., Soncrant, T. T., Ingram, D. K., and Brossi, A. (1995) *Med. Res. Rev. 15*, 3−31.
16. Zhu, X. D., Cuadra, G., Brufani, M., Maggi, T., Pagella, P. G., Williams, E., and Giacobini, E. (1996) *J. Neurosci. Res. 43*, 120−126.
17. Aldridge, W. N., and Reiner, E. (1972) in *Frontiers of Biology* (Neuberger, A., and Tatum, E. L., Eds.) Vol. 26, p 125, North-Holland Publishing, Amsterdam.
18. Perola, E., Cellai, L., Lamba, D., Filocamo, L., and Brufani, M. (1997) *Biochim. Biophys. Acta 1343*, 41−50.
19. Sussman, J. L., Harel, M., Frolow, F., Varon, L., Toker, L., Futerman, A. H., and Silman, I. (1988) *J. Mol. Biol. 203*, 821−823.
20. Otwinowski, Z., and Minor, W. (1997) *Methods Enzymol. 276*, 307−326.
21. Collaborative Computational Project Number 4 (1994) *Acta Crystallogr. D50*, 760−763.
22. Sussman, J. L., Lin, D., Jiang, J., Manning, N. O., Prilusky, J., Ritter, O., and Abola, E. E. (1998) *Acta Crystallogr. D54*, 1078−1084.
23. Brünger, A. T. (1996) *X-PLOR. Version 3.851. A system for X-ray crystallography and NMR*, Yale University Press, New Haven, CT.
24. Jones, T. A., Zhou, J.-Y., Cowan, S. W., and Kjeldgaard, M. (1991) *Acta Crystallogr. A47*, 110−119.
25. Engh, R. A., and Huber, R. (1991) *Acta Crystallogr. A47*, 392−400.
26. Kleywegt, G. J., and Jones, T. A. (1994) *Acta Crystallogr. D50*, 178−185.
27. Dougherty, D. A. (1996) *Science 271*, 163−168.
28. Scrutton, N. S., and Raine, A. R. C. (1996) *Biochem. J. 319*, 1−8.
29. Wlodek, S. T., Clark, T. W., Scott, L. R., and McCammon, J. A. (1997) *J. Am. Chem. Soc. 119*, 9513−9522.
30. Szegletes, T., Mallender, W. D., and Rosenberry, T. L. (1998) *Biochemistry 37*, 4206−4216.
31. Wriggers, W., and Schulten, K. (1997) *Biophys. J. 73*, 624−639.
32. Young, R. G., Lawson, D., and Rayment, I. (1995) *Biophys. J. 68*, S44−S49.

BI982723P